J Wood Sci (1999) 45:98–105

ORIGINAL ARTICLE

Xiu-Ming Diao · Takeshi Furuno · Minoru Fujita

Digital image analysis of cross-sectional tracheid shapes in Japanese softwoods using the circularity index and aspect ratio*

Received: May 22, 1998 / Accepted: September 22, 1998

Abstract Image analysis was used in this study to develop a faster, more objective method for quantitatively measuring tracheid shapes on cross section. The morphological features were measured automatically using the circularity index and aspect ratio based on the skeletonized images. The rectangular and hexagonal similarities were introduced to evaluate the tracheid shapes. The results for 18 species of Japanese softwoods showed that the difference in tracheid shapes among the species could be successfully estimated using the quantitative method. In addition, the boundary of latewood might be evaluated based on the change in circularity indexes.

Key words Tracheid shape · Circularity index · Aspect ratio · Shape similarity · Image analysis

Introduction

Image-processing techniques have been widely used in quantitative analyses of cells or particle shapes in various fields, for example, automatic classification of crops according to morphology,[1] determining the optimum operating condition of the impactor particles of cement powder,[2] and predicting the concentration of airborne dust in woodworking chambers.[3] For studying wood anatomy, measurements of cell shapes have become possible. Gonzalez and Wintz[4] and Levine[5] noted that several stand edge detectors are available for delineation of cell boundaries using computer image-processing techniques. As a new approach, image processing based on the distance transform[6] was used for quantitative assessment of wood cell boundaries. Recently, element angles (angles between two radial walls) of tracheids and variation of shape in a single annual ring were investigated using fast Fourier transform (FFT) image analysis.[7,8]

In our previous study[9] the morphological features of cross-sectional vessel shapes for 47 Japanese species were analyzed quantitatively using image processing. The circularity index has proven to be a useful means for assessing cell shape difference between solitary pores and pore multiples. The variability of cross-sectional tracheid shapes, especially earlywood, is not large; but recently some studies have shown that there is an important effect of cross-sectional tracheid shapes on the anisotropy of wood properties.[10,11] Therefore, studying the morphological features of tracheids is necessary to explain the anisotropy or to predict various properties of wood using theoretical models. In this study we characterized the morphological features of tracheid shapes on cross sections and their changes within an annual ring using a circularity index and an aspect ratio by an image-processing technique.

Materials and methods

Microscopy

Samples from 18 Japanese softwoods were used in this study, as shown in Table 1. Measurements of morphological features were made by different annual ring widths. Cross sections, 10–20 μm thick, were cut with a sliding microtome, stained with 1% aqueous safranine, and mounted on glass slides. Photographs were taken continuously along the radial direction from earlywood to latewood in every annual ring with a 20× objective and an FK2.5× ocular. The magnification of the photographs was 364.

X.-M. Diao · T. Furuno (✉)
Faculty of Science and Engineering, Shimane University, Matsue 690-8504, Japan
Tel. +81-852-32-6563; Fax +81-852-32-6123
e-mail: t-furuno@riko.shimane-u.ac.jp

M. Fujita
Division of Forest and Biomaterials Science, Graduate School of Agriculture, Kyoto University, Kyoto 606-8502, Japan

*The abstract of this study was presented at the 48th annual meeting of the Japan Wood Research Society, Shizuoka, April 1998

Table 1. Morphological features of tracheids in earlywoods for 18 Japanese softwoods

Species	Scientific names	RW (mm)	LP (%)	CI_{AV}	λ_{AV}	S_T	S_H	No.
Momi[a]	*Abies firma* Sieb. et Zucc.	1.27	14.60	0.782 (0.094)	1.532 (0.746)	94.09 (4.70)	92.10 (6.59)	3930
Todomatsu	*Abies sachalinensis* Mast.	1.17	10.05	0.728 (0.157)	1.708 (0.699)	92.18 (9.24)	89.66 (11.45)	2088
Hinoki	*Chamaecyparis obtusa* Endl.	4.03	2.46	0.822 (0.119)	1.733 (0.502)	88.48 (5.10)	94.57 (7.59)	8703
Sawara	*Chamaecyparis pisifera* Endl.	1.19	6.05	0.819 (0.091)	1.753 (0.848)	90.47 (3.51)	96.09 (4.44)	3761
Sugi	*Cryptomeria japonica* D. Don	1.97	7.48	0.829 (0.087)	1.638 (0.744)	90.82 (3.02)	95.23 (3.08)	10994
Karamatsu	*Larix kaempferi* Carr.	1.79	15.65	0.821 (0.081)	1.613 (0.469)	91.15 (3.66)	96.41 (3.97)	3486
Ezomatsu	*Picea jezoensis* Carr.	1.25	16.36	0.826 (0.130)	1.582 (0.724)	87.93 (6.10)	93.92 (8.91)	2868
Akamatsu[a]	*Pinus densiflora* Sieb. et Zucc.	1.75	25.03	0.841 (0.075)	1.566 (0.501)	89.96 (3.68)	94.87 (3.10)	3880
Himekomatsu	*Pinus parviflora* Sieb. et Zucc.	1.14	19.16	0.797 (0.093)	1.650 (1.014)	93.64 (2.50)	94.25 (3.27)	2747
Kuromatsu	*Pinus thunbergii* Parl.	1.01	18.57	0.822 (0.084)	1.598 (0.435)	91.99 (3.26)	93.80 (3.07)	8700
Inumaki	*Podocarpus macrophylla* D. Don	1.82	11.82	0.777 (0.073)	1.444 (0.425)	95.84 (3.57)	90.54 (4.91)	8458
Togasawara	*Pseudotsuga japonica* Beissn.	3.83	24.33	0.803 (0.050)	1.623 (0.081)	93.02 (2.85)	94.74 (1.24)	3771
Koyamaki	*Sciadopitys verticillata* Sieb. et Zucc.	0.75	14.81	0.767 (0.072)	1.518 (0.561)	96.68 (3.04)	90.81 (4.41)	3020
Ichii	*Taxus cuspidata* Sieb. et Zucc.	0.73	17.16	0.817 (0.076)	1.691 (0.562)	91.11 (3.26)	96.52 (3.01)	3297
Nezuko	*Thuja standishii* Carr.	1.37	23.05	0.819 (0.104)	1.705 (0.783)	89.55 (4.71)	95.30 (5.71)	3793
Hiba	*Thujopsis dolabrata* Sieb. et Zucc.	1.03	10.21	0.821 (0.078)	1.549 (0.509)	91.88 (3.31)	95.95 (3.41)	2913
Kaya	*Torreya nucifera* Sieb. et Zucc.	0.75	20.96	0.763 (0.072)	1.513 (0.567)	94.62 (3.14)	90.31 (4.21)	2385
Tsuga	*Tsuga sieboldii* Carr.	1.31	25.77	0.776 (0.066)	1.509 (0.454)	96.26 (3.10)	91.30 (4.13)	3160

The data in parentheses are standard deviations.
RW, average value of five annual ring widths; LP, average latewood percentages for five annual rings; CI_{AV}, average circularity indexes; λ_{AV}, average aspect ratios; S_T, rectangular similarities; S_H, hexagonal similarities; No, number of measured tracheids.
[a]The number of annual rings is 11.

Image analysis

The photographs were digitized by an image scanner (flatbed type, IX-4015; Canon) with an image resolution of 64 dpi. A Macintosh 8100/80AV personal computer system was used for storing and analyzing the digital images. When input, the horizontal coordinate in a cathode-ray tube (CRT) display corresponds to the tangential direction of the original image. The monochromatic images with a good contrast were 400 × 600 pixels and 256 gray levels. The magnification of 364 for the photographs corresponded to 1.09 μm/pixel of the original images. The morphological features of individual tracheids in the digitized images were measured using the software NIH (National Institutes of Health, USA) Image/ppc 1.56b77.

Because copyfilms were used during photographing, photographs with a clear boundary between the cell wall and cell lumen were obtained. Monochromatic images with good contrast were easily binarized. The binary cell wall image produced was then spatially filtered to remove high-frequency noises. An opening process was used to remove small foreground objects and irregularities in the larger object boundaries. Then a closing process of one pixel was used to remove small holes from the remaining foreground objects (cell wall).

Although the cell lumina can be clearly distinguished, the boundaries between cells are less obvious. To discern these boundaries on the assumption that the cell boundaries are midway between adjacent cells, we used a shrinkage technique that is similar to the distance transform. A skeleton of the binary cell wall image with a single pixel approximates the position of the middle lamella between adjacent cell walls. It is possible to measure various parameters of the cells from these images, such as the cross-sectional area and perimeter. An exception occurs when making measurements of cells near the ray cells. When shrinkage processing was used, the shrinkage of the ray cells caused deviation of cell shapes near ray cells. This was due to a precondition of shrinkage processing that lay on the assumption that the double wall thickness was the same. Thus, measurements of the cell lumen were carried out near the ray cells without the shrinkage processing.

Feature extraction

Morphological features of particles can be described by many parameters, such as area, perimeter, Heywood diameter, maximum length, maximum breadth, aspect ratio, and circularity index as a shape factor. In this study, the circularity indexes and aspect ratios as the important morphological factors were measured to evaluate quantitatively the shapes of tracheids. The circularity index is defined by the following formula.[12]

$$CI(\lambda) = \frac{4\pi A}{C^2} \tag{1}$$

where CI is the circularity index, C is the perimeter, A is the area, and λ is the aspect ratio expressed by the ratio of Feret's radial diameter (D_R^F) and Feret's tangential diameter (D_T^F). The CI is 1.0 for any circle and 0.785 for any perfect square, and their aspect ratios are 1.0.

Ohgoshi et al.[13] used the relation between the circularity index and the aspect ratio to evaluate the shapes of

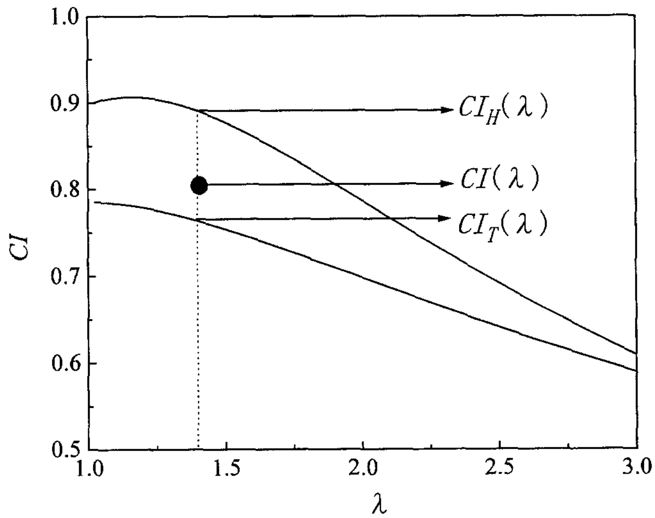

Fig. 1. Relation between the circularity indexes of rectangles or hexagons and the aspect ratios. *CI*, circularity index; λ, aspect ratio; $CI(\lambda)$, circularity index of a tracheid; $CI_H(\lambda)$, circularity index of a hexagon; $CI_T(\lambda)$, circularity index of a rectangle

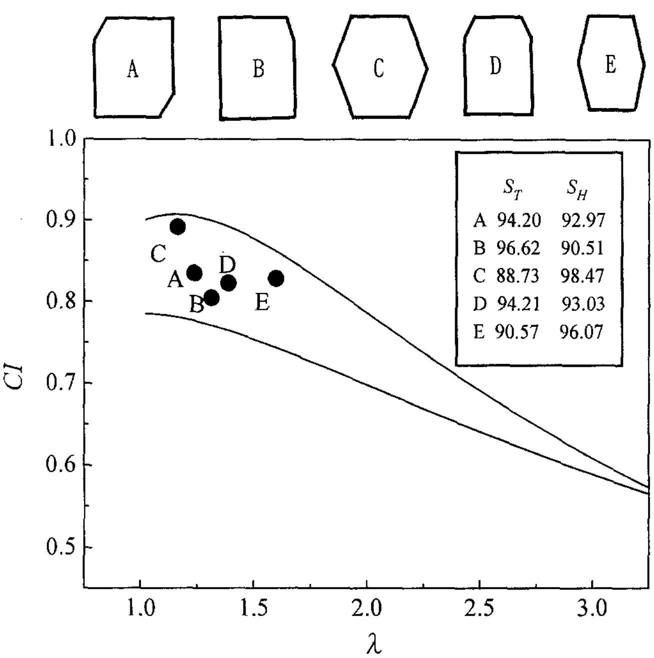

Fig. 2. Relation between the circularity index (*CI*) and aspect ratio (λ) for various models. S_T, rectangular similarity; S_H, hexagonal similarity

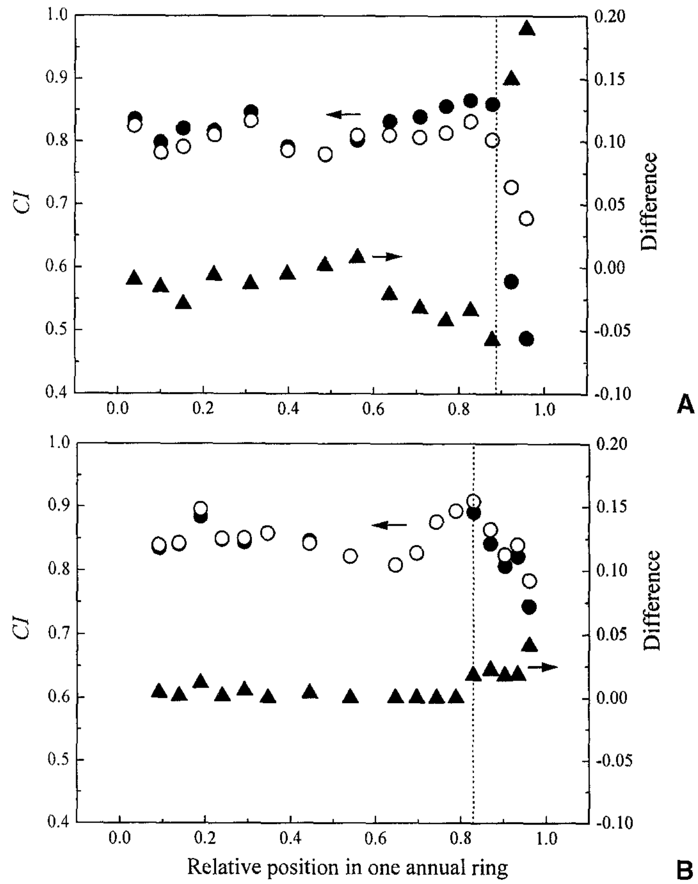

Fig. 3. Comparison of circularity indexes (*CI*) between the lumen and middle lamella boundaries. *Solid circles*, lumen boundary; *open circles*, middle lamella boundary; *solid triangles*, differences in circularity indexes between lumen and middle lamella boundaries. **A** Ichii (*Taxus cuspidata* Sieb. et Zucc.). Ring width is 0.45 mm and latewood percentage 15.35%. **B** Sugi (*Crytomeria japonica* D. Don). Ring width is 1.87 mm and latewood percentage 18.96%. *Dotted lines*, boundary of latewood according to Mork's definition

bordered-pit membrane pores of softwoods by the image analysis system. Fujiwara[14,15] also used the circularity index and aspect ratio (D_R^F/D_T^F) to analyze the changes in fiber shapes during fiber differentiation in hardwoods. Usually when an effect of tracheid shapes on cross sections on the wood properties is discussed, rectangular or hexagonal models are used. It is necessary to evaluate whether the shapes of tracheids in any species are more similar to a rectangle or a regular hexagon. The circularity index of a tracheid is compared with that of a rectangle or a hexagon with the aspect ratio (λ) of a tracheid. A similarity to a rectangle or a regular hexagon was introduced into evaluations of tracheid shapes. The rectangular similarity (S_T) and hexagonal similarity (S_H) were calculated by the following formula:

$$S_T = \left[1 - \left|CI(\lambda) - CI_T(\lambda)\right|\right] \times 100 \quad (2)$$

$$S_H = \left[1 - \left|CI(\lambda) - CI_H(\lambda)\right|\right] \times 100 \quad (3)$$

From this formula it is understood that if the circularity index $[CI(\lambda)]$ of the tracheid is equal to that of a rectangular model $[CI_T(\lambda)]$ or a regular hexagonal model $[CI_H(\lambda)]$, S_T or S_H is 100. This shows that the shape of a tracheid is the same as a rectangle or a regular hexagon.

The circularity indexes of a rectangle $[CI_T(\lambda)]$ and a regular hexagon $[CI_H(\lambda)]$ were calculated based on the aspect ratio (λ) of a tracheid using the following formula:

$$\text{Rectangle: } CI_T(\lambda) = \frac{\pi}{\lambda + 2 + \frac{1}{\lambda}} \quad (4)$$

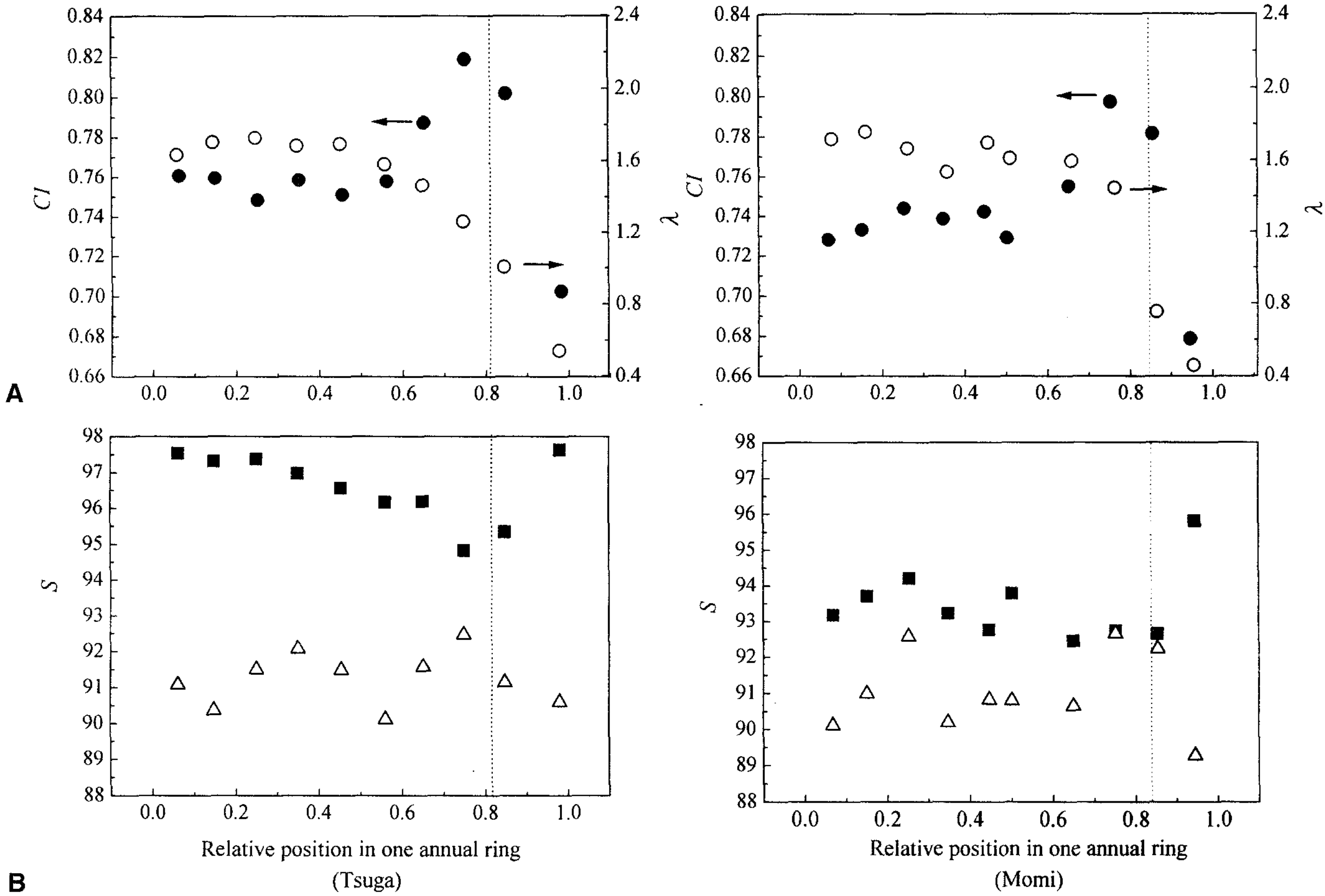

Fig. 4. Change of circularity index (*CI*), aspect ratio (λ), and shape similarity (*S*) in tsuga (*Tsuga sieboldii* Carr, *left*) and momi (*Abies firma* Sieb. et Zucc, *right*). *Solid circles*, circularity index; *open circles*, aspect ratio; *solid squares*, rectangular similarity; *open triangles*, hexagonal similarity; *dotted lines*, boundary of latewood according to Mork's definition

Hexagon:

$$\theta = 2\arcsin\frac{\lambda\left(1+\sqrt{1+3\lambda^2}\right)}{2\left(1+\lambda^2\right)} \quad (5)$$

$$CI_{\mathrm{H}}(\lambda) = \frac{\pi}{9}\left(2\sin\frac{\theta}{2} + \sin\theta\right) \quad (6)$$

where θ is an element angle[16] (the angle between two radial walls) obtained from the aspect ratio (Eq. 5). Figure 1 shows the relations between the circularity indexes of rectangles or hexagons and the aspect ratios.

To help understand the shape similarity concept, the various possible models of earlywood tracheids are shown in Fig. 2. Models A, B, and D were assumed to be tracheids near rays. Models C and E were assumed to be tracheids in earlywood. Their rectangular and hexagonal similarities were estimated as shown in Fig. 2. The results show that the shapes of the models can be evaluated quantitatively on the basis of the shape similarity.

In addition, when the areas, perimeters, and aspect ratios of tracheids were measured, the coordinates of tracheids in a computer display were also measured. Therefore, one annual ring was divided into 10 parts on the basis of the coordinates from earlywood to latewood to obtain the distribution of circularity indexes and the shape similarities.

Accuracy of a circularity index

In a previous paper[9] we made circles with various diameters of about 5–37 pixels using a paint software to discuss the effects of digitizing processing on the accuracy of a circularity index. According to the results obtained, the circularity index of the circle increased rapidly as the circle diameter increased. If the diameter of a circle was larger than 35 pixels, the relative error of the circle perimeters was less than 3%, and that of the circularity indexes of the circles was less than 5%. To reduce the errors that resulted from the digitizing process, the Heywood diameters ($d = \sqrt{4A/\pi}$) of tracheids were estimated. The circularity indexes of tracheids were corrected on the basis of the Heywood diameters using the regression formula of a measured circularity index and its diameter ($CI = 1.039 - 0.315/\ln d$).

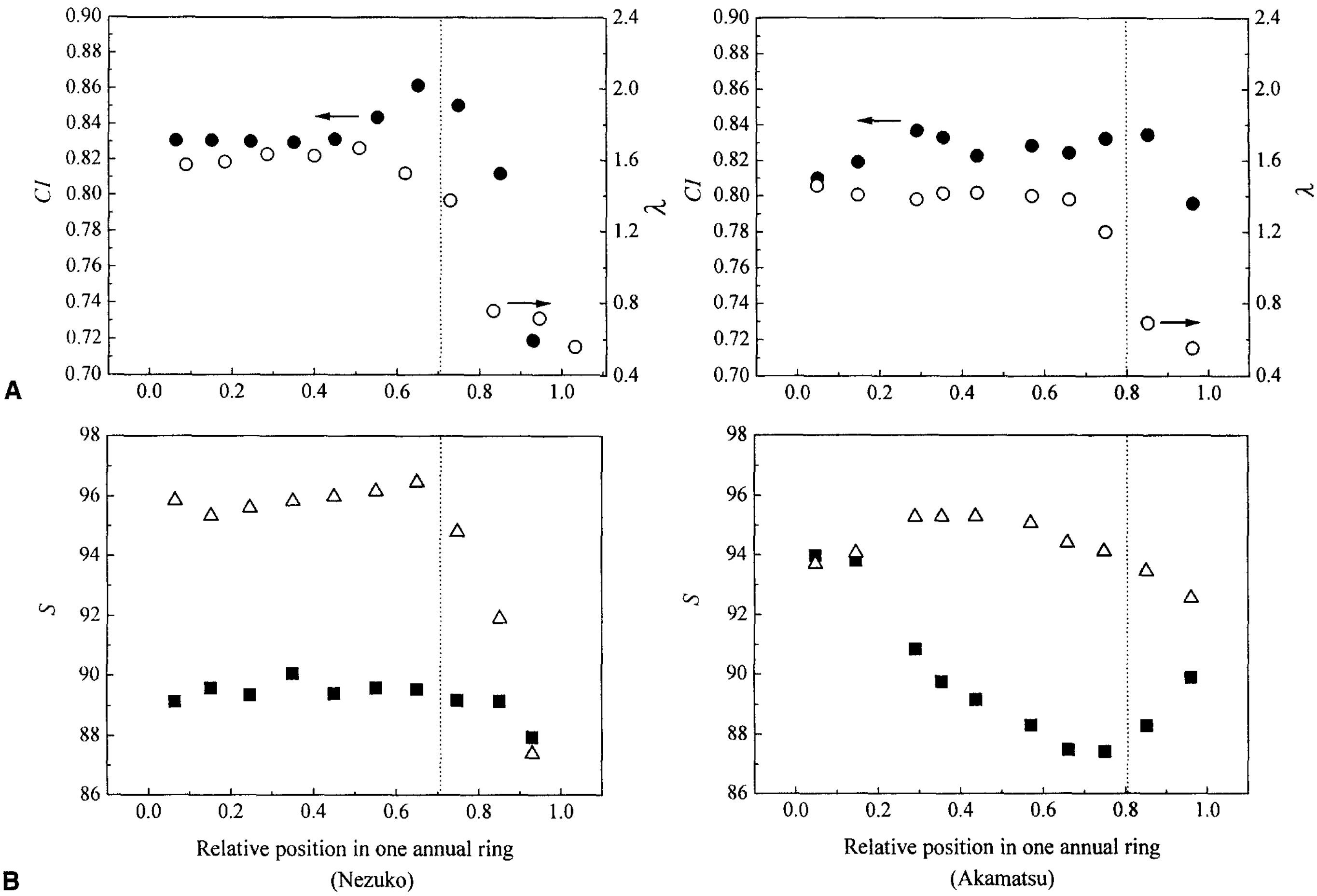

Fig. 5. Change of circularity index (*CI*), aspect ratio (λ), and shape similarity (*S*) in nezuko (*Thuja standishii* Carr, *left*) and akamatsu (*Pinus densiflora* Sieb. et Zucc, *right*). Symbols are the same as in Fig. 4

To determine the effects of a threshold gray level during binarizing on the circularity indexes, the average values of about 100 earlywood tracheids were measured in the different threshold gray levels for three species: sugi (*Cryptomeria japonica* D. Don), todomatsu (*Abies sachalinensis* Mast.), and akamatsu (*Pinus densiflora* Sieb. et Zucc.). There are few variations of the circularity indexes from threshold values of 100–200. This is due to monochromatic photographs having a good contract when a copyfilm was used. For all monochromatic images, the threshold gray level was about 150 with binary processing.

Results and discussion

Shapes of middle lamella boundary and lumen

To compare the difference of shapes between the middle lamella boundary (MLB) and the lumen, their circularity indexes were measured. Figure 3 shows the shape variations of the MLB and lumen for ichii (*Taxus cuspidata* Sieb. et Zucc.) and sugi (*Cryptomeria japonica* D. Don). The results show the larger differences in the circularity indexes of the MLB and lumen for ichii and the small differences for sugi. Because the cell wall thickness in the earlywoods is small, the effects of cell corners are relatively small. Generally, as the cell walls thicken, the effects of cell corners become larger. On the other hand, tracheid diameters may affect tracheid shape. Peachey and Osborne[6] indicated that the difference in shapes between the MLB and lumen appeared as an increase in cell wall thickness. The cross-sectional shapes of tracheids are the shapes of MLB in this study.

Averages of circularity index, aspect ratio, and shape similarities

It was reported that the shapes of tracheids have a larger effect in earlywood than in latewood in terms of the properties of the wood, such as shrinkage and Young's modulus; the effects of the cell wall structure itself become greater as the cell walls thicken.[10,16] Table 1 shows the morphological features of tracheids, such as the average circularity indexes and aspect ratios and the rectangular and hexagonal similarities measured in earlywood of five annual ring widths. For akamatsu (*Pinus densiflora* Sieb.

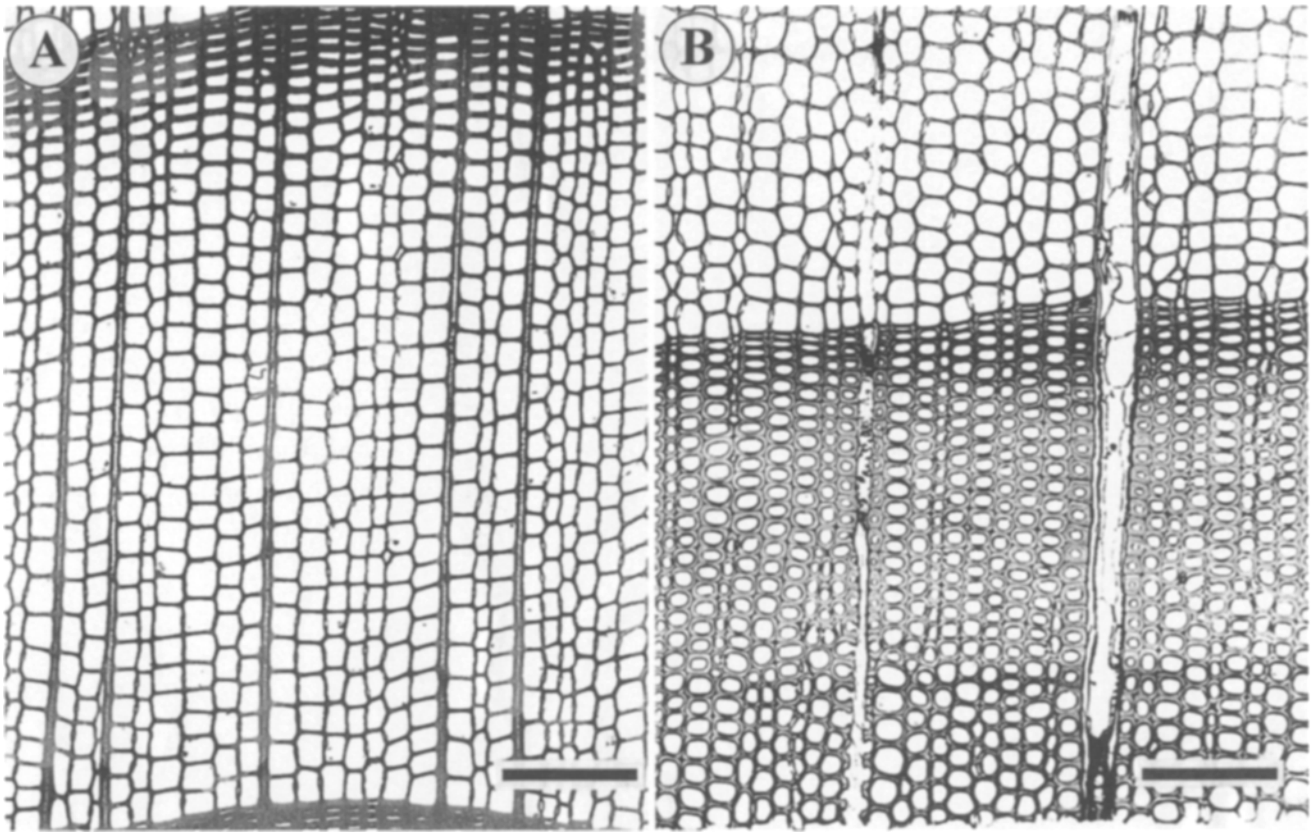

Fig. 6. Microphotographs of transverse sections of momi (*Abies firma* Sieb. et Zucc) (**A**) and akamatsu (*Pinus densiflora* Sieb. et Zucc.) (**B**). Bars 200 μm

et Zucc.) and todomatsu (*Abies sachalinesis* Mast.), the averages of the circularity indexes are 0.841 and 0.728; these are maximum and minimum values, respectively, compared with those of other species. For all species, the averages of the aspect ratios vary from 1.50 to 1.75. Based on the standard deviations, the variations in aspect ratios are large.

The rectangular and hexagonal similarities for each tracheid were calculated according to Eqs. (2) and (3). The averages and standard deviations are shown in Table 1 for 18 Japanese softwood species. Because there is a difference between the rectangular and hexagonal similarities, it is suggested that similarity is a useful tool for evaluating the shape of cross-sectional tracheids. Comparing their shape similarities, the rectangular similarities are larger than the hexagonal ones for momi (*Abies firma* Sieb. et Zucc.), inumaki (*Podocarpus macrophyllus* D. Don), koyamaki (*Sciadopitys verticillata* Sieb. et Zucc.), kaya (*Torreya nucifera* Sieb. et Zucc.), and tsuga (*Tsuga sieboldii* Carr.). The other species have larger hexagonal than rectangular similarities. The differences in tracheid shapes among species could be evaluated from the results of the two types of shape similarity. It is important to explain the production of wood anisotropy and to predict various properties of wood using theoretical models.

Change in circularity index and shape similarity within an annual ring

Generally, the variation in tracheid shapes can be examined by visual observation, and it is usually believed that tracheid shapes are similar to hexagons in earlywood and to rectangles in latewood. To evaluate this variation quantitatively, we measured the changes in circularity index and shape similarity within an annual ring. Typical results are shown in Figs. 4 and 5. Figure 4B shows that the rectangular similarities are larger than the hexagonal similarities in tsuga (*Tsuga sieboldii* Carr.) and momi (*Abies firma* Sieb. et Zucc.). It is concluded that the tracheid shapes of the two species are closer to rectangles. In contrast, the tracheid shapes are closer to hexagons for nezuko (*Thuja standishii* Carr.) and akamatsu (*Pinus densiflora* Sieb. et Zucc.) (Fig. 5B). The shapes of many tracheids may be similar to models A, B, and D in Fig. 2 because the circularity index of momi is close to that of a rectangle (Fig. 4B). Figures 4A and 5A demonstrated that there are larger circularity indexes in the transition zone than those in earlywood and latewood. Jagels and Dyer[17] studied the tracheid shape change of red spruce within an annual ring. Their results showed that the boundary between earlywood and latewood could be evaluated based on the peak of the circularity index. In Figs. 4

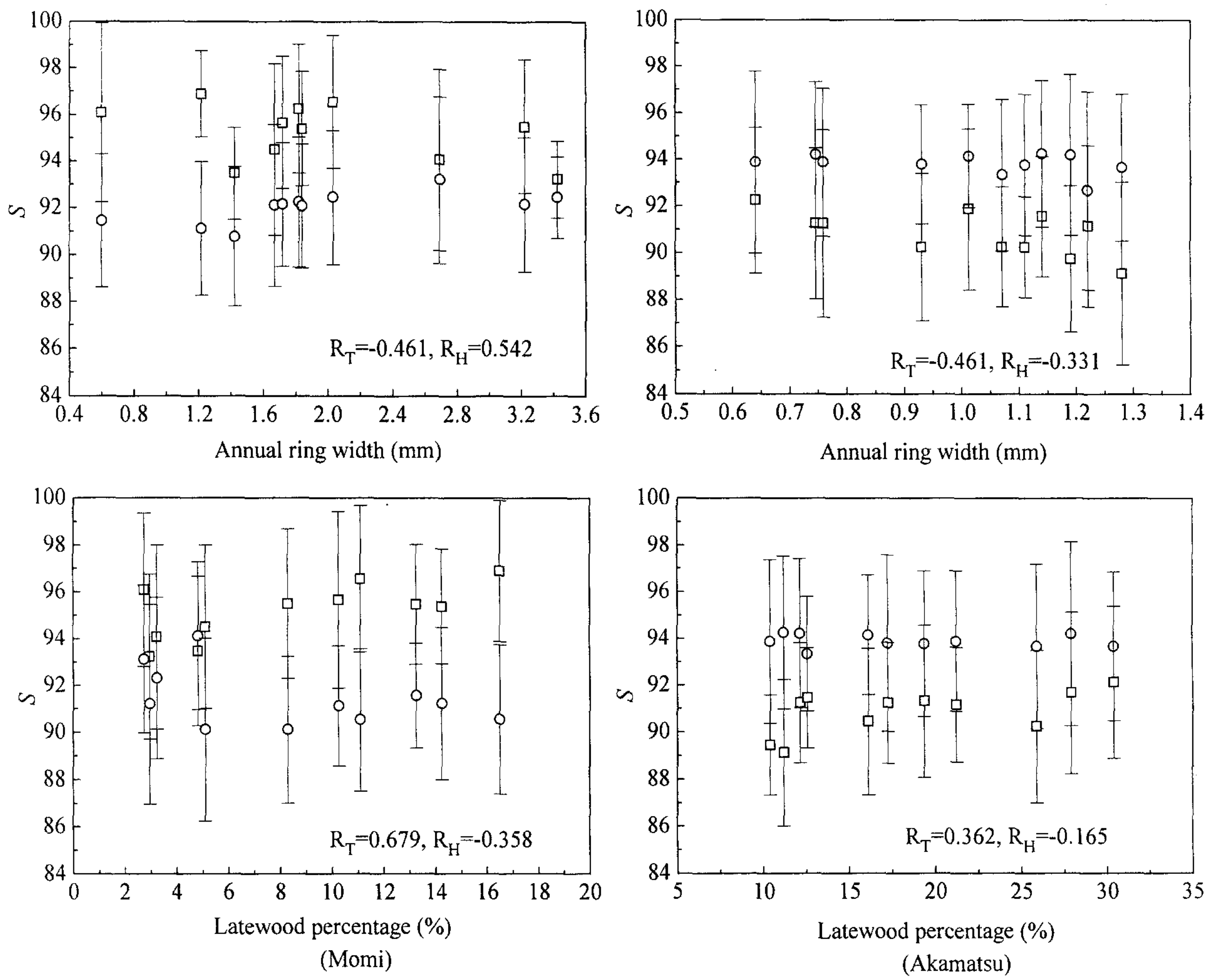

Fig. 7. Relation between shape similarities (S) and annual ring width as well as the latewood percentage for momi (*Abies firma* Sieb. et Zucc.) (*left*) and akamatsu (*Pinus densiflora* Sieb. et Zucc.) (*right*). *Open squares*, rectangular similarity; *open circles*: hexagonal similarity. Vertical lines represent standard deviations. R_T and R_H, correlation coefficients

and 5, the dotted lines show the boundary of latewood obtained according to Mork's definition.[18,19] There is a good agreement between the boundary of latewood based on Mork's definition and the peak of the circularity index rather than the shape similarities.

Effects of annual ring width and latewood percentage

To determine the effects of annual ring widths and latewood percentages on the similarities of tracheids, we measured the shape similarities for momi (*Abies firma* Sieb. et Zucc.) and akamatsu (*Pinus densiflora* Sieb. et Zucc.) in 11 annual ring widths. According to the visual observation (Fig. 6), there are clear differences in tracheid shape between the two species.

Figure 7 shows the relation between the shape similarity and annual ring width and the latewood percentage for momi and akamatsu. The shape similarity, as the average of all tracheids in every ring and its standard deviation, were obtained. The annual ring width and latewood percentage were measured, when measuring the shape similarity of tracheids in every ring. There was little correlation between the rectangular similarity and annual ring width because there are smaller correlation coefficients at the 0.95 confidence level. There is a higher correlation between rectangular similarity and latewood percentage for momi. Here the contribution of the latewood tracheids with the larger rectangular similarities become larger as the latewood percentages increase. With this increase, it is evident that the number of latewood tracheids with higher rectangular similarity increases. The results for akamatsu show that the rectangular similarity and hexagonal similarity have little change as the latewood percentage increases. This is because the shapes of latewood tracheids were similar to hexagons, although the latewood percentage increased. In addition, based on the results for akamatsu in Fig. 5, it was proved that the tracheid shapes in latewood are similar to hexagons because the hexagonal similarities in latewood have large values. For other species, the effects of the annual ring width and the latewood on the shape similarity cannot be discussed because of few number of their annual rings.

Conclusion

Using image analysis techniques, the morphological properties of tracheids on cross section for 18 species of Japanese softwoods were measured quantitatively based on the circularity index and aspect ratio. The rectangular and hexagonal similarities were introduced to evaluate the tracheid shapes. The difference in tracheid shapes among species could be successfully estimated using this quantitative method. In addition, the boundary of latewood might be evaluated using the change in circularity index. However, using the shape similarity concept, it would be difficult to reconstruct the models of tracheid shapes because the cell wall dimensions (e.g., cell wall length and the element angle) as important parameters of tracheid shape could not be determined. It is necessary to measure automatically the dimensions and element angles of cell walls using the FFT method.

References

1. Travis AJ, Hirst DJ, Chesson A (1996) Automatic classification of plant cells according to tissue type using anatomical features obtained by the distance transform. Ann Bot 78:325–331
2. Taniguchi S, Kano T, Nakamura M (1994) Improvement of particle shape and particle size distribution of cement by high-velocity pneumatic double-stage impactor (in Japanese). J Soc Mater Sci 43:1444–1450
3. Fujii Y, Nemoto H, Sawada Y, Okumura S, Ikegiwa H (1997) Prediction of the concentration of airborne dust in the woodworking chamber. I. Time changes of the concentration and distribution of particles in free falling (in Japanese). Mokuzai Gakkaishi 43:203–209
4. Gonzalez RC, Wintz P (1987) Digital image processing. Addison-Wesley, Reading, MA, p 82
5. Levine M (1985) Computer vision in man and machine. McGraw-Hill, New York, p 124
6. Peachey TC, Osborne CF (1990) The measurement of wood cell parameters using the distance transform. Wood Fiber Sci 22:388–403
7. Midorikawa Y, Fujita M, Saiki H (1995) Quantitative evaluation of cross-sectional cell shapes by the Fourier transform image analysis (in Japanese). In: Abstracts of the 40th anniversary conference of the JWRS, Tokyo, p 36
8. Midorikawa Y, Fujita M (1997) Quantitative evaluation of cross-sectional cell shapes by the Fourier transform image analysis. III (in Japanese). In: Abstracts of the 47th annual meeting of the JWRS, Kochi, p 19
9. Diao X, Furuno T, Uehara T (1997) Quantitative morphological evaluation of cross-sectional vessel shapes in hardwoods using image processing. Mokuzai Gakkaishi 43:709–716
10. Watanabe U, Norimoto M, Fujita M (1998) Transverse shrinkage anisotropy of coniferous wood investigated by the power spectrum analysis. J Wood Sci 44:9–14
11. Watanabe U, Norimoto M, Fujita M (1998) Transverse shrinkage of coniferous wood cells examined using replica method and power spectrum analysis. Holzforschung 52:200–206
12. Takagi M, Shimoda H (1993) Image analysis handbook. Tokyo University Press, Tokyo, pp 580–581
13. Ohgoshi M, Nakato T, Sadoh T (1982) Quantitative evaluation of bordered-pit membrane pores of softwoods by the image-analysis system (in Japanese). Mokuzai Gakkaishi 28:583–589
14. Fujiwara T (1993) Changes of fiber shapes during fiber differentiation in hardwoods. I. Three-dimensional analysis of fiber shapes in keyaki and tochinoki (in Japanese). Mokuzai Gakkaishi 39:509–513
15. Fujiwara T (1993) Changes of fiber shapes during fiber differentiation in hardwoods. II. Three-dimensional shapes of wood fibers in sendan and variation of cross-sectional dimensions of fibers measured on a transverse section of the wood (in Japanese). Mokuzai Gakkaishi 39:1219–1225
16. Norimoto M (1987) Specific Young's modulus and quality of coniferous wood (in Japanese). Mokuzai Gakkaishi 33:545–551
17. Jagels R, Dyer M (1983) Morphometric analysis applied to wood structure. I. Cross-sectional cell shape and area change in red spruce. Wood Fiber Sci 15:376–386
18. Mork E (1928) Die qualitäat des fichtenholzes unter besonderer rücsichtnahme auf schleif- und papierholz. Papier Fabrikant 26:741–747
19. Denne MP (1988) Definition of latewood according to Mork (1928). IAWA Bull 10(1):59–62